Review Article

Journal of Molecular Microbiology and Biotechnology

J Mol Microbiol Biotechnol 2016;26:119–137
DOI: 10.1159/000440805

Published online: March 10, 2016

Structure and Function of the Unusual Tungsten Enzymes Acetylene Hydratase and Class II Benzoyl-Coenzyme A Reductase

Matthias Boll[a] Oliver Einsle[b] Ulrich Ermler[c] Peter M.H. Kroneck[d]
G. Matthias Ullmann[e]

[a]Fakultät für Biologie/Mikrobiologie and [b]Lehrstuhl Biochemie, Institut für Biochemie, Albert-Ludwigs-Universität Freiburg, Freiburg, [c]Max-Planck-Institut für Biophysik, Frankfurt, [d]Fachbereich Biologie, Universität Konstanz, Konstanz, and [e]Computational Biochemistry, Universität Bayreuth, Bayreuth, Germany

Key Words
Acetylene hydratase · Benzoyl-coenzyme A reductase · Tungsten enzymes

Abstract
In biology, tungsten (W) is exclusively found in microbial enzymes bound to a bis-pyranopterin cofactor (bis-WPT). Previously known W enzymes catalyze redox oxo/hydroxyl transfer reactions by directly coordinating their substrates or products to the metal. They comprise the W-containing formate/formylmethanofuran dehydrogenases belonging to the dimethyl sulfoxide reductase (DMSOR) family and the aldehyde:ferredoxin oxidoreductase (AOR) families, which form a separate enzyme family within the Mo/W enzymes. In the last decade, initial insights into the structure and function of two unprecedented W enzymes were obtained: the acetaldehyde forming acetylene hydratase (ACH) belongs to the DMSOR and the class II benzoyl-coenzyme A (CoA) reductase (BCR) to the AOR family. The latter catalyzes the reductive dearomatization of benzoyl-CoA to a cyclic diene. Both are key enzymes in the degradation of acetylene (ACH) or aromatic compounds (BCR) in strictly anaerobic bacteria. They are unusual in either catalyzing a nonredox reaction (ACH) or a redox reaction without coordinating the substrate or product to the metal (BCR). In organic chemical synthesis, analogous reactions require totally nonphysiological conditions depending on Hg^{2+} (acetylene hydration) or alkali metals (benzene ring reduction). The structural insights obtained pave the way for biological or biomimetic approaches to basic reactions in organic chemistry.

Introduction

With the exception of nitrogenases, the group of Mo and W enzymes are widely distributed in all domains of life and catalyze a large variety of oxo- or hydroxyl-group transfer reactions, thereby mostly acting as oxidoreductases. All of them bind the transition metal via one or two pyranopterins with or without a linkage to nucleotides, and are referred as mono- or bis-molybdopterin (MPT)/tungstopterin (WPT). Depending on the nature of the cofactor, the additional proteinogenic or inorganic ligands at the metal and the overall amino-acid sequence similarities, four different Mo/W enzyme families are distinguished: the xanthine oxidase (XO), sulfite oxidase (SO), dimethyl sulfoxide reductase (DMSOR) and aldehyde:ferredoxin oxidoreductase (AOR) families. In mem-

KARGER

E-Mail karger@karger.com
www.karger.com/mmb

1464–1801/16/0263–0119$39.50/0

Prof. Dr. Matthias Boll
Institute of Biology II, University of Freiburg
Schänzlestrasse 1
DE–79104 Freiburg (Germany)
E-Mail matthias.boll@biologie.uni-freiburg.de

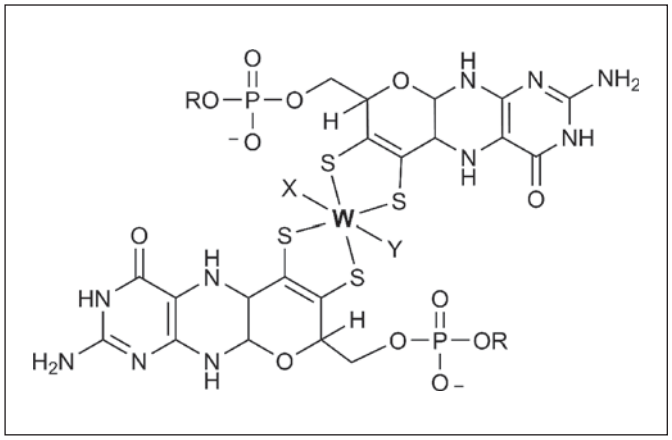

Fig. 1. The bis-WPT cofactor. DMSOR family: X = Cys-SH or Se-Cys; Y = inorganic O or S atom; R = GMP. AOR family: X = O (AORs) or Cys-SH (class II BCRs); an additional Y-ligand was not identified in AORs but is present in class II BCRs (see fig. 7); R = H.

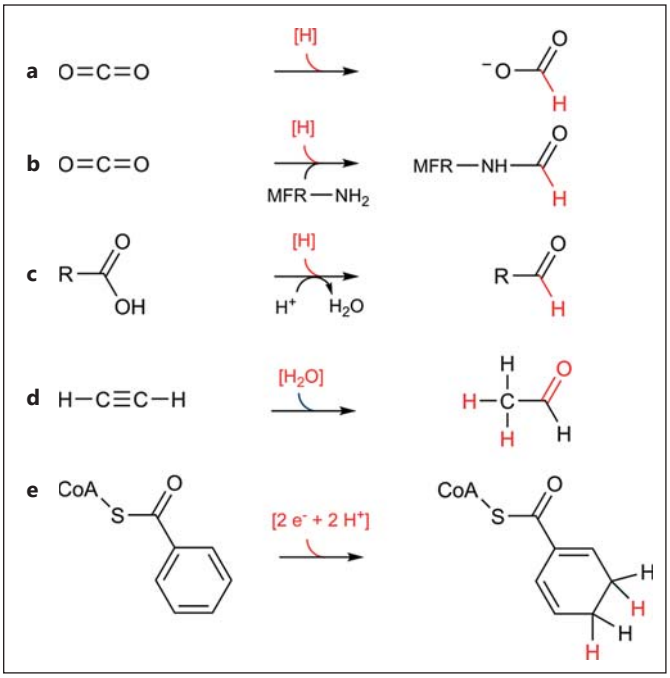

Fig. 2. Reactions catalyzed by WPT-containing enzymes. **a** FDH. **b** Formylmethanofuran dehydrogenase (MFR). **c** AOR. **d** ACH. **e** BCR. **a**, **b**, **d** DMSOR family. **c**, **e** AOR family. For AORs, the biological function is rather the oxidation of aldehydes than the reduction of carboxylic acids (shown in **d**).

bers of the XO and SO families, the transition metal is coordinated by the dithiolene group of a single pyranopterin and varying inorganic S/O atoms or a cysteine (SO family). In the DMSOR and AOR families, the Mo/W atoms are always coordinated by four dithiolene sulfur atoms of the bis-MPT/WPT cofactors and a large variety of proteinogenic or inorganic ligands (fig. 1). For recent general reviews of Mo/W enzymes see previously published studies [Bevers et al., 2009; Hille, 2013; Hille et al., 2014; Pushie et al., 2014; Romao, 2009; Schwarz et al., 2009].

In most cases, Mo/W enzymes have a preference for either of the respective transition metals [Andreesen and Makdessi, 2008; L'vov et al., 2002; Pushie et al., 2014; Rothery and Weiner, 2015]. However, there are also reports on the presence/exchange of both metals in formate dehydrogenases (FDHs) [Hartmann et al., 2014]. The XO and SO family members exclusively contain Mo. The DMSOR family mainly comprises Mo enzymes, but a few members prefer W over Mo: (a) FDHs from some obligately anaerobic microorganisms [Hartmann et al., 2014]; (b) formylmethanofuran dehydrogenases from various methanogenic archaea [Vorholt and Thauer, 2002], and (c) acetylene hydratase (ACH) from strictly anaerobic bacteria [Seiffert et al., 2007; Ten Brink, 2014]; in the AOR family, exclusively W enzymes have been found and include (d) AORs from hyperthermophilic archaea and mesophilic bacteria with varying specificities for their respective aldehyde substrate [Kletzin and Adams, 1996; Roy and Adams, 2002], and (e) the recently identified class II benzoyl-CoA reductases (BCRs) from strictly anaerobic bacteria [Boll et al., 2014]. With the exception of ACH, all currently known W enzymes catalyze redox reactions at very low standard redox potentials with $E^{\circ\prime}$ values of –430 mV (FDHs), –560 to –610 mV (AORs) and –622 mV (BCRs; fig. 2). This property is in line with the general observation that biologically relevant (IV/V/VI) redox transitions occur at lower redox potentials in W than in Mo complexes; consequently, W is generally preferred over Mo in low-potential redox catalysis [Andreesen and Makdessi, 2008; L'vov et al., 2002; Pushie et al., 2014; Roy and Adams, 2002]. However, there are also a few exceptions, e.g. the XO family member 4-hydroxybenzoyl-CoA reductase catalyzes a reaction at $E^{\circ\prime} < -500$ mV [Unciuleac et al., 2004] and a Mo(V/IV) redox transition at $E^{\circ\prime} = -500$ mV was determined [Boll et al., 2001].

Almost all Mo/W enzymes catalyze two-electron transfer redox reactions with ACH as the only exception catalyzing a 'true' nonredox reaction [Hille, 2013; Pushie et al., 2014]. Notably, the Mo-containing pyrogallol-phloroglucinol transhydroxylase (DMSOR family) does not catalyze a net redox reaction; however, the overall reaction can be divided into two consecutive oxidation/re-

duction partial reactions [Boll et al., 2005]. The two-electron redox reactions normally involve oxo- or hydroxo transfer with the substrate or product being directly coordinated to the Mo/W via an oxygen atom [Hille, 2013; Pushie et al., 2014]. The only exceptions appear to be W-containing BCRs, which contain an occupied W ligation shell without the option of additional substrate or product binding [Weinert et al., 2015].

In this review, we summarize our current knowledge of ACH and class II BCR, two bis-WPT-containing enzymes that have only recently been studied in detail. The biochemical, structural and mechanistic data obtained provide initial insights into their intricate reactions and expand our knowledge of the variability of Mo-/W-dependent catalysis in biology.

Acetylene Hydratase

Biological Function of ACH

Acetylene (C_2H_2) is well known as an inhibitor of microbial processes. It can interact with the active site of numerous metal-dependent enzymes, such as nitrogenase, hydrogenase, ammonia monooxygenase, methane monooxygenase, assimilatory nitrate reductase or nitrous oxide reductase [Hyman and Arp, 1988]. Acetylene is a minor trace gas in today's Earth atmosphere and can be used as carbon and energy source by distinct microorganisms [Abbasian et al., 2015; Oremland and Voytek, 2008]. The W and Fe-S enzyme ACH was originally discovered from *Pelobacter acetylenicus* by Schink [1985] (EC 4.2.1.112) and studied in great detail over the past three decades. ACH is a hydrolyase, it catalyzes the addition of one molecule of water to the C≡C triple bond of acetylene to form acetaldehyde, which is then further converted to ethanol and acetate (equations 1, 2):

$$C_2H_2 + H_2O \rightarrow CH_3CHO \qquad \Delta G_o' = -111.9 \text{ kJ per mol acetaldehyde} \quad (1)$$

The subsequent disproportionation of acetaldehyde to ethanol and acetate yields by far less energy, but is still exergonic:

$$2\ CH_3CHO + H_2O \rightarrow CH_3CH_2OH + CH_3COO^- + H^+ \qquad \Delta G_o' = -17.3 \text{ kJ/mol acetaldehyde} \quad (2)$$

Clearly, the conversion of C_2H_2 by ACH is distinct from the only other known enzymatic reaction of acetylene, the reduction to ethylene (C_2H_4) by nitrogenase [Stewart et al., 1967]. Notably, the addition of one molecule of water to C_2H_2 is formally not a redox reaction; however, ACH activity depends on the presence of a strong reducing agent, e.g. Ti(III) citrate or Na^+ dithionite [Meckenstock et al., 1999]. Cyanide (CN^-) as well as nitric oxide (NO) act as inhibitors; organic nitriles (R-CN) and isonitriles (R-NC) did not react with ACH, neither did propine ($CH_3C{\equiv}CH$) nor structurally related compounds, such as HOOC-C≡CH, HOOC-C≡C-COOH or $HOCH_2$-C≡CH [Seiffert, 2007].

General Properties

ACH from *P. acetylenicus* is so far the only ACH that has been purified and studied by biochemical, spectroscopic, crystallographic and computational methods. The first purification of ACH was published in 1995 [Rosner and Schink, 1995], followed by a high-resolution crystal structure [Seiffert et al., 2007] and heterologous expression and site-directed mutagenesis of several amino acids located at the active site [Ten Brink et al., 2011]. ACH was isolated from the soluble fraction of *P. acetylenicus* cells as a monomer [73 kDa/SDS-PAGE; 83.5 kDa/MALDI mass spectrometry (MS)]. Activity of ACH depended on the presence of tungstate, or molybdate, in the growth media. Maximum activity of the enzyme reduced with 2 mM Ti(III) citrate was observed at pH 6.0–6.5, the temperature optimum was around 50°C [2 mM Ti(III) citrate; pH 7.0], and the K_m for acetylene was 14 μM [Rosner and Schink, 1995].

ACH is a member of the DMSOR family based on its amino acid sequence and its crystal structure. When purified under N_2/H_2 (94/6% v/v) atmosphere, it contains 0.4–0.5 mol W/mol enzyme and 3.7–3.9 mol Fe/mol enzyme (inductively coupled plasma MS) [Meckenstock et al., 1999; Rosner and Schink, 1995; Ten Brink et al., 2011], and the bis-WPT-guanine-dinucleotide cofactor. When isolated under N_2/H_2 (94/6% v/v) atmosphere, ACH was silent in electron paramagnetic resonance (EPR) spectroscopic analysis; EPR spectra of the enzyme reduced with dithionite showed the typical signal of a low-potential ferredoxin-type $[4Fe\text{-}4S]^{+1}$ cluster (g_z = 2.048, g_y = 1.939, g_x = 1.920 [Meckenstock et al., 1999]). Upon oxidization of ACH with one equivalent hexacyanoferrate(III) $\{[Fe(CN)_6]^{3-}\}$, the spectra revealed the signal of a W(V) center (g_x = 2.007, g_y = 2.019, g_z = 2.048). The dependence of ACH activity on the applied redox potential was investigated by potentiometry, giving a standard midpoint potential of –410 mV for the [4Fe-4S] cluster [Meckenstock et al., 1999]. The enzyme activity had a midpoint potential around –340 mV, indicating that ACH was active in the W(IV) state, whereas the redox state of the iron-sulfur center appeared to be less important for enzyme activity.

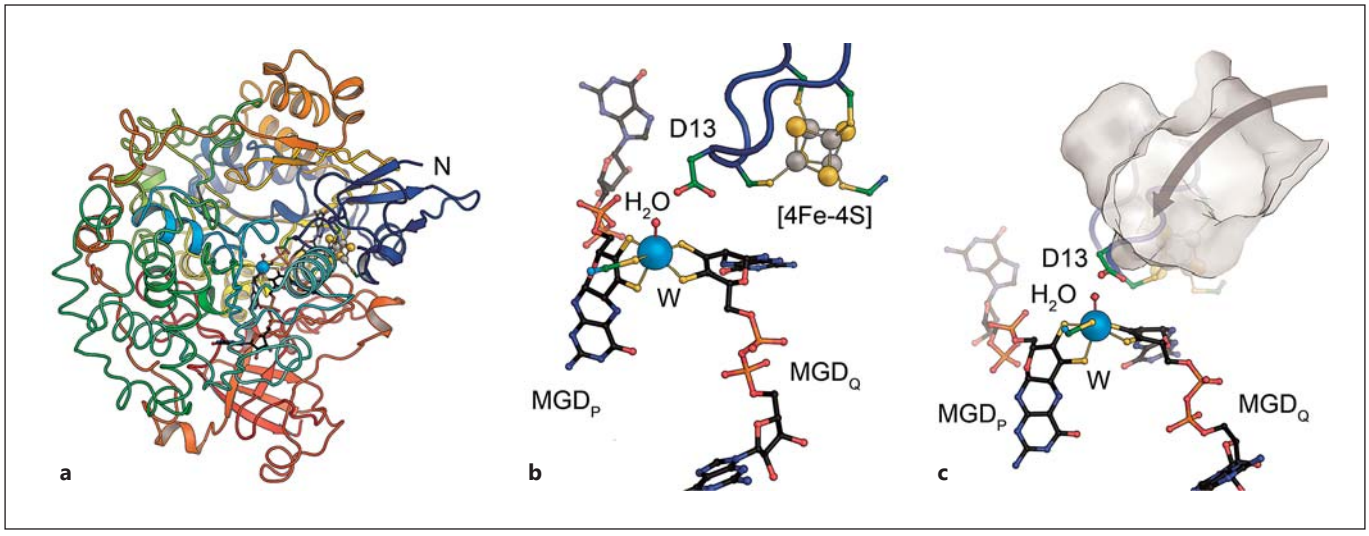

Fig. 3. X-ray structure of ACH of *P. acetylenicus* (1.26 Å resolution). **a** Overall structure. **b** Active site showing the W center, the nearby [4Fe-4S] cluster and the crucial residue Asp13 (D13). **c** Active site showing the hydrophobic pocket responsible for substrate binding. PDB ID code 2E7Z [Seiffert et al., 2007].

Notably, a Mo-dependent active form of ACH could be obtained from *P. acetylenicus;* activity with both Mo or W has also been demonstrated for another member of the DMSOR family [Stewart et al., 2000]. Growth of *P. acetylenicus* in medium containing only trace amounts of tungstate (2 vs. 800 nM in the original tungstate medium) and elevated amounts of molybdate (2 μM vs. 6 nM) led to a Mo form of ACH (ACH-Mo) which was 10 times less active than the original ACH-W but still converted acetylene to acetaldehyde at a rate of 1.9 versus 14.8 μmol/min/mg of the original ACH-W. ACH-Mo contained 0.45–0.51 mol Mo/mol enzyme and 2.7–3.1 mol Fe/mol enzyme; W was absent. The EPR spectrum of ACH-Mo, as isolated in the absence of dioxygen, showed a weak signal from a Mo(V) center ($g_x = 1.978$, $g_y = 1.99$, $g_z = 2.023$), which increased in size upon addition of $[Fe(CN)_6]^{3-}$. Dithionite reduced samples of ACH-Mo revealed again the signal of the ferredoxin-type [4Fe-4S] cluster as found in ACH-W. Furthermore, only minor differences in the circular dichroism spectroscopy data of the two forms of ACH were detected. Attempts to replace W by V failed [Abt, 2001; Ten Brink, 2010].

Structural Properties of ACH

A first high-resolution X-ray structure (1.26 Å) of ACH was published in 2007 (PDB ID 2E7Z) [Seiffert et al., 2007]. The crystallization of ACH was achieved under a N_2/H_2 (94/6% v/v) atmosphere at 20°C using the sitting drop vapor diffusion method [Einsle et al., 2005]. Despite the minor differences in the circular dichroism spectroscopy data of ACH-W and ACH-Mo, only the former formed protein crystals suitable for X-ray analysis.

Overall Structure

ACH is a monomer of 730 amino acids, containing a bis-WPT guanine dinucleotide cofactor moiety and a [4Fe-4S] cluster. The two cofactors are buried deep inside a four-domain fold, as typically observed for enzymes of the DMSOR family (fig. 3a) [Seiffert et al., 2007, 2008]. Domain I (residues 4–60) harbors the [4Fe-4S] cluster, ligated by the four cysteine residues Cys9, Cys12, Cys16 and Cys46. Domains II (residues 65–136 and 393–542) and III (residues 137–327) have an αβα-fold with homologies to the NAD-binding fold of dehydrogenases. Each of these two domains provides hydrogen bonds, required to bind one of the WPT guanine dinucleotides (generally referred to as MGD, MPT guanine dinucleotide), as they are identical in Mo- or W-containing cofactors of the DMSOR family). The interactions are mainly provided by variable loop regions at the C-terminal ends of the strands of a parallel β-sheet. The coordination of the two MGD cofactors is completed by domain IV (residues 590–730), which consists mainly of a seven-strand β-barrel fold [Seiffert et al., 2007].

The overall structure of ACH and the position of the cofactors, with the two MGDs (referred to as MGD_P and

MGD_Q) in an elongated conformation and the [4Fe-4S] cluster close to the MGD_Q are similar to all other structures of members of the DMSOR family published so far. However, the access from the surface of the protein towards the active site, consisting of the W center coordinated by the two MGDs with the [4Fe-4S] cluster in close proximity, is unique for an enzyme of the DMSOR family. In all structures of this family of enzymes published so far, the access funnel starts at the pseudo twofold axis between domains II and III. A shift in the loop region of residues 327–335 towards the surface of the protein and further rearrangements of the residues 336–393 block this entrance in ACH. In other enzymes, e.g. nitrate reductases and FDHs, this loop region separates the [4Fe-4S] cluster from the Mo/W site. In ACH, the shift of this loop opens a new access funnel towards the W center at the intersection of domains I, II and III, allowing the substrate to approach the W site from a completely different direction compared with other enzymes of the DMSOR family [Seiffert et al., 2007].

The Active Site

While the overall fold of ACH is remarkably similar to those observed in the enzymes of the DMSOR family, major structural rearrangements are found at the active site. The W center in its reduced W(IV) state is coordinated by the four sulfur atoms of the dithiolene moieties of the P_{MGD} and Q_{MGD} cofactors, and by one sulfur atom of a cysteine residue (Cys141). The sixth ligand position is occupied by a tightly coordinated oxygen atom at a distance of 2.04 Å from the W ion. Due to a rotation of the P_{MGD} cofactor, the geometry of the coordination in ACH is not square pyramidal or trigonal prismatic, as typically found in enzymes of this family [Dobbek and Huber, 2002], but resembles more an octahedral or trigonal antiprismatic coordination geometry (fig. 3b) [Seiffert et al., 2007].

The access funnel opened by a shift in the loop region of residues 327–335 ends in a ring of six bulky hydrophobic residues (Ile14, Ile113, Ile142, Trp179, Trp293 and Trp472) that form a small hydrophobic pocket directly above the oxygen ligand and an adjacent aspartate residue (Asp13; fig. 3c). Asp13, a direct neighbor of the [4Fe-4S] coordinating Cys12, forms a tight hydrogen bond of 2.41 Å to the oxygen ligand of the W ion. Although it has not yet been possible to solve a crystal structure with acetylene or an inhibitor bound, an acetylene molecule docked computationally to the ACH structure gave an excellent fit in the pocket of the hydrophobic ring with its carbon atoms positioned directly above the oxygen ligand and the carboxylic acid group of Asp13 [Seiffert et al., 2007].

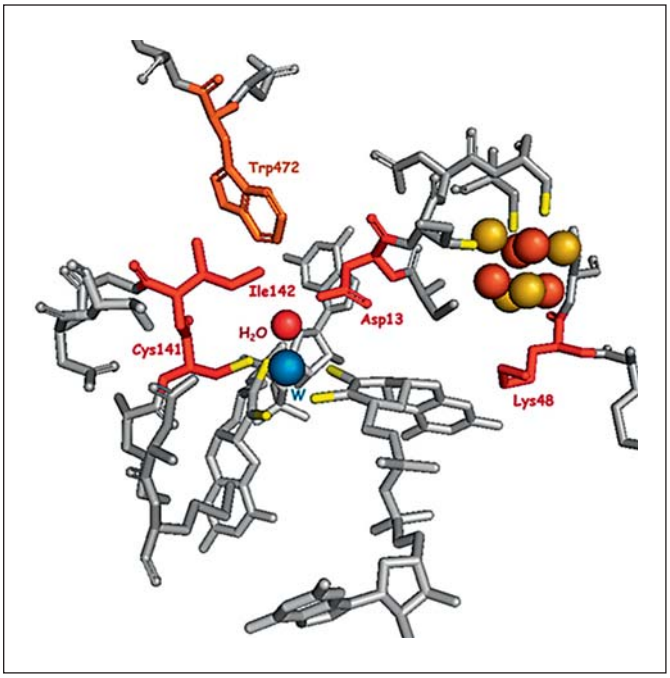

Fig. 4. Variants of ACH. Biochemically characterized variants (D13A, D13E, K48A, C141S and I142A) are marked in red; the variant W472A (marked in orange) could not be isolated [Ten Brink, 2010; Ten Brink et al., 2011].

The nature of the oxygen ligand of the W center is crucial for deriving the ACH reaction mechanism. The bond length of 2.04 Å observed in the X-ray structure was between the values expected for a hydroxo ligand (1.9–2.1 Å) and a coordinated water molecule (2.0–2.3 Å). Seiffert et al. [2007] chose a water molecule, since the close proximity of the heavy scatterer W may distort the distance observed in the X-ray data by Fourier series termination and a simulation of this effect resulted in a true ligand distance of 2.25 Å.

Site-Directed Mutagenesis and Mechanistic Aspects

The development of a successful protocol for the heterologous expression of ACH in *Escherichia coli* allowed for site-directed mutagenesis studies [Ten Brink et al., 2011]. Overall, when related to its W content, the activity of the heterologously produced ACH was nearly identical to that of the native enzyme purified from *P. acetylenicus*. Three amino acids at the active site were exchanged by site-directed mutagenesis: Asp13, Lys48 and Ile142 (fig. 4). Asp13 forms a hydrogen bond to the oxygen ligand (OH^- or H_2O) of the W center and is assumed to be catalytically important in the sense that it activates the

oxygen atom for the addition to the C≡C triple bond. The mutation of Asp13 to alanine (D13A variant) resulted in a dramatic loss of activity (0.2 vs. 2.6 μmol/min/mg; wild type), while the mutation of Asp13 to glutamate (D13E variant) had little effect (2.5 μmol/min/mg). These results underline the important role of the carboxylic acid group, as discussed below.

Residue Lys48 is located between the [4Fe-4S] cluster and the MGD_Q cofactor (fig. 3, 4). In other enzymes of the DMSOR family, this residue is involved in electron transfer between the two cofactors [Dobbek and Huber, 2002]. As expected given that the reaction of ACH does not involve net electron transfer, the exchange of Lys48 against alanine did not affect catalysis.Finally, Ile142 is part of the hydrophobic pocket that is expected to form the substrate-binding cavity at the end of the access tunnel towards the active site (fig. 3, 4). Its mutation to alanine resulted in a strong loss of activity, in support of the idea that the cavity within the hydrophobic ring is the substrate-binding site of ACH. However, until now, numerous experiments to locate the binding of the substrate acetylene in crystallography or by spectroscopic methods have not been successful [Seiffert, 2007; Ten Brink, 2010].

Computational Studies

The mechanism of ACH has been investigated in several computational studies [for review, see Ten Brink, 2014]. One important prerequisite for calculating an accurate mechanism is the correct assignment of the protonation state of the active site residues. This is best done by electrostatic calculations [Bashford and Karplus, 1990; Ullmann and Knapp, 1999]. In these calculations, the shift of the protonation energy of a titratable residue due to the protein environment compared to the protonation energy of a titratable group free in aqueous solution is calculated using the Poisson-Boltzmann equation [Ullmann and Bombarda, 2014]. The shift in protonation energy is caused by two effects: (i) the protein environment can stabilize, or destabilize, charged groups by specific interactions such as hydrogen bonds or salt bridges, and (ii) the titratable group resides in a different solvation environment within the protein compared to the situation of an isolated titratable group in aqueous solution. In fact, in the protein, the titratable group is at least partially shielded from the solvent, which lowers the reaction field stabilization and thus destabilizes the charged state of the titratable group. However, a protein has usually several interacting titratable groups. In order to obtain a titration of a particular group, the protonation probability has to be calculated by a thermodynamic average over all possible protonation states of the protein [Bashford and Karplus, 1990], which can be achieved by a Monte Carlo averaging for large proteins [Beroza et al., 1991; Ullmann and Ullmann, 2012]. If two or more groups interact strongly and titrate in the same pH range, the corresponding titration curves can adopt a nonsigmoid shape [Klingen et al., 2006]. In extreme cases, even nonmonotonic titration curves can be observed [Onufriev et al., 2001; Sudmeier and Reilley, 1964]. This behavior can be interpreted as a pH dependence of the protonation energy, and thus the pK_a value, of a particular group in the protein [Bombarda and Ullmann, 2010]. Such a pH-dependent protonation energy can, however, also be found for residues that titrate at very different pH but interact strongly. A consequence of this finding is that a pK_a value that is read from the midpoint of a pH titration curve of a group cannot always be associated with a defined protonation energy. Instead, the protonation energy has to be considered pH dependent if several titratable groups interact strongly [Ullmann and Bombarda, 2013].

One remarkable result of the calculated titration curves for ACH was the finding that the COOH group of Asp13, which is located right at the active site of the enzyme close to the W center (fig. 3, 4), did lose its proton at high pH [Seiffert et al., 2007]. A free energy calculation of the protonation energy indicates that the protonated state of Asp13 is stabilized by about 9 kcal/mol at pH 7 [Ullmann, unpubl. results]. This finding is not too surprising, since the active site is very well shielded from the solvent which would destabilize the negatively charged (i.e. deprotonated) state of Asp13. Moreover, the electrostatic potential at the active site is already overall negative due to the presence of the W center [charge of –1 due to the oxidation state W(+IV) and five negatively charged sulfur ligands] and the reduced iron sulfur cluster (which has a total charge of –3). In another theoretical study, Liao et al. [2010] estimated a pK_a value of 6.3 for Asp13 using PROPKA [Bas et al., 2008]. However, the PROPKA algorithm used does not take into account either the charge effect of the W center nor that of the iron sulfur cluster, which will most likely lead to an underestimation of the pK_a value of Asp13.

The crystal structure of ACH solved at high resolution suggests two alternative reaction mechanisms [Seiffert et al., 2007]. Depending on the nature of the oxygen ligand of the W center (OH^- or H_2O), either a nucleophilic addition of H_2O to the acetylene C≡C triple bond or an electrophilic Markovnikov-type addition has been proposed. Notably, in both suggested mechanisms, the substrate

acetylene does not interact directly with the W ion, but is located in the pocket formed by a hydrophobic ring interacting with the oxygen ligand which is activated by the W(IV) center and Asp13. The crystal structure favors the coordination of a water molecule over the coordination of a hydroxo ligand, due to a W-O bond distance of about 2.25 Å. A bound water molecule could gain a partially positive net charge by the proximity of the protonated Asp13, turning it into an electrophile that could directly attack the C≡C triple bond. In several computational studies [for review, see Ten Brink, 2014], this second shell mechanism was investigated. However, in all studies only reaction pathways with unrealistically high barriers were obtained. Therefore, different mechanisms were suggested for ACH based on these computational studies involving a direct binding of the substrate acetylene to W. Especially in the work of Liao et al. [2010], a mechanism with reasonably low barriers was suggested. Notably, Asp13 was assumed to be deprotonated in these calculations, most likely an unrealistic assumption as discussed above. In the mechanism proposed by Liao et al. [2010], acetylene forms a η^2-complex with the W ion by displacing the water ligand. The energy barrier for this step was not calculated in this study. The water molecule that was displaced by acetylene attacks the η^2-acetylene complex forming a vinyl anion, and a water proton is transferred to the Asp13 carboxylate group. In a subsequent step, the resulting vinyl anion is protonated by Asp13 yielding the corresponding vinyl alcohol. The tautomerization of the vinyl alcohol to acetaldehyde most likely occurs spontaneously in solution after the release from the active site or even at the active site. In any case, this latter reaction will proceed spontaneously with a low energy barrier, perhaps with the assistance of water and Asp13 in case this reaction occurs at the active site. The mechanism that was found by pure QM cluster calculations [Liao et al., 2010] was recently also investigated by QM/MM calculations [Liao and Thiel, 2012, 2013], which led to similar conclusions.

Even though the mechanism involving a η^2-complex of acetylene with W may appear plausible, a direct or indirect proof of this mechanism is still lacking. Different reaction pathways that have not been discovered yet may exist. Moreover, the transition barrier for the replacement of water by acetylene has not been calculated yet. In the energetic considerations, it must also be considered that the concentration of water is much higher than that of acetylene. A crucial point in the understanding of the mechanism of ACH will be the determination of the protonation state of Asp13. Thus, more theoretical and experimental work will be required before the quest for the mechanism of ACH can be considered to be finished [Ten Brink, 2014].

Distribution of ACH-Related Enzymes

The genus *Pelobacter* comprises strictly anaerobic fermenting, Gram-negative Deltaproteobacteria. The best investigated species within this genus are *Pelobacter carbinolicus* and *P. acetylenicus*. The genome of *P. carbinolicus* has been sequenced; this organism is closely related to *P. acetylenicus*. *Pelobacter* species feed only on a narrow substrate range. *P. carbinolicus* and *P. acetylenicus* degrade acetoin, 2,3-butandiol, ethylene glycol *(P. carbinolicus)* or acetylene *(P. acetylenicus)* in pure culture, or ethanol in coculture with a syntrophic partner. The metabolism of all these substrates includes acetaldehyde as central intermediate, which was proposed to be the ecological specialization or niche of these bacteria [Schink, 2006; Schmidt et al., 2014].

In principle, the electron-rich C≡C triple bond and the excellent solubility in water make acetylene a suitable substrate for microorganisms. The first report on bacteria living with acetylene was published as early as 1932 [Birch-Hirschfeld, 1932]. Almost 50 years later, *Norcadia rhodochrous* was aerobically grown with acetylene as sole source of carbon and energy in the presence of dioxygen; in addition, ACH activity was detected in cell-free extracts from *Rhodococcus A1* grown with acetylene under fermentative conditions [de Bont and Peck, 1980; Kanner and Bartha, 1979]. Anaerobic oxidation of acetylene to CO_2 was found in enrichment cultures from estuarine sediments. Two groups of bacteria were identified: (i) fermenting bacteria converted acetylene to acetaldehyde, which they transformed to acetate and ethanol, and (ii) sulfate-reducing bacteria further oxidized both ethanol and acetate to CO_2 [Culbertson et al., 1988]. According to these authors, the morphology of the bacteria was similar to that of *P. acetylenicus* [Schink, 1985]. Rosner et al. [1997] described aerobic acetylene-degrading bacteria from soil samples. Two isolates were assigned to the species *Rhodococcus opacus*, two others to *Rhodococcus ruber* and *Gordonia* sp. ACH activity was present in cell-free extracts of *R. opacus* and required Ti(III) citrate, whereas in experiments with cell-free extracts of *R. ruber* and *Gordonia* sp. no reductant had to be added. However, cross reactivity with antibodies raised against ACH from strictly anaerobic fermenting organism *P. acetylenicus* was not found, and the authors concluded that ACHs represent a biochemically heterogeneous group of enzymes. In this context, when performing activity or microbial growth experiments with commercially available acetylene gas,

one should recall that this gas usually contains acetone. In growth experiments with the aerobic strain MoAcy2 *(Gordonia alkanivorans),* a zinc-dependent enzyme (M_r 40 kDa) could be enriched from cell extracts which appeared to be an oxygen-tolerant ACH. However, when using purified acetylene gas (grade 2.6; passage through concentrated sulfuric acid) [Hyman and Arp, 1988], formation of acetaldehyde from acetylene was no longer observed [Fischer et al., unpubl. results].

Recently, a more systematic survey was conducted on the presence of ACH activity. Anoxic samples from chemically diverse field sites were assayed for their ability to consume acetylene. Over incubation periods of 10–80 days, selected samples from 7 of the 13 tested sites displayed significant C_2H_2 removal. No significant formation of ethylene was noted in these incubations, and C_2H_2 consumption was attributed to ACH rather than to nitrogenase activity. The lag phase was explained by selecting and enriching bacteria that thrive on acetylene. This would mean that acetylene-fermenting bacteria were rather scarce in the original samples. Furthermore, the authors tried to amplify genes coding for ACH from DNA extracted from the sediment and water samples. The use of primers synthesized from the ACH gene of *P. acetylenicus* resulted in 63 PCR products out of 645 environmental samples (9.8%). Since ACH-like genes could not be amplified in all samples exhibiting ACH activity, it was argued that the primer may have been overly specific for the ACH gene of *P. acetylenicus* [Miller et al., 2013]. Early BLASTP searches showed that ACH isolated from *P. acetylenicus* had the highest similarity to a putative MPT oxidoreductase of the hyperthermophilic archaeon *Archaeoglobus fulgidus* (protein accession No. NP_070031); the sequence identity was about 35%. Five of the 15 cysteine residues of ACH were highly conserved and 4 of them showed a sequence motif [C-x-x-C-x-x-x-C-$(x)_n$-C], representing a motif for a [4Fe-4S] site. In view of the results of the BLASTP searches, *A. fulgidus* was tested for ACH activity at 80°C using the thermostable alcohol dehydrogenase from *Sulfolobus solfataricus*. Neither the crude extract nor partially purified fractions from *A. fulgidus* showed any significant ACH activity [Abt, 2001].

Class II Benzoyl-CoA Reductase

Biological Function of BCRs

For a long time, it had generally been accepted that the complete degradation of aromatic compounds requires molecular oxygen as cosubstrate for ring hydroxylation and cleavage catalyzed by mono- and dioxygenases. However, in the past decades, an increasing number of aromatic compound-degrading anaerobes have been isolated from sediments of rivers, lakes, seas or aquifers contaminated with aromatic compounds. These facultative or obligate anaerobes belong to nearly all physiological classes, including denitrifying, metal oxide-respiring, sulfate-reducing and fermenting bacteria, as well as bacteria with an anoxygenic photosynthesis [Boll et al., 2014; Carmona et al., 2009; Fuchs et al., 2011].

In anaerobic bacteria, the vast majority of monocyclic aromatic growth substrates are converted to the central intermediate benzoyl-CoA by channelling reactions of the peripheral catabolism. Benzoyl-CoA or analogues with hydroxy, methyl or halogen substituents at the ring serve then as substrates for dearomatizing reductases that reduce the benzene moiety to the cyclic, conjugated cyclohexa-1,5-diene-1-carbonyl-CoA (dienoyl-CoA; fig. 2e) or analogs with substituents of it [Boll, 2005; Boll et al., 2014; Buckel et al., 2014; Carmona et al., 2009; Fuchs et al., 2011]. The two-electron reduction of aromatic rings to cyclic dienes is known as a basic reaction in organic chemical synthesis referred to as Birch reduction [Birch, 1944; Zimmerman, 2012]. It uses alkali metals dissolved in ammonia to form solvated electrons as donors; alcohols serve as weak proton source. It proceeds in single electron transfer and protonation step with the first electron transfer forming a highly reactive radical anion transition state. Considering the nonphysiological conditions of Birch reductions, it was surprising that such a reaction can be accomplished in a biological environment [Buckel et al., 2014; Kung et al., 2010; Mobitz and Boll, 2002].

The reduction potential of the benzoyl-CoA/dienoyl-CoA couple is with $E^{\circ\prime} = -622$ mV among the most negative ones known in biology [Kung et al., 2010]. This low two-electron reduction potential can be rationalized by the resonance-stabilized aromatic π-electron system. As there is no common biological electron donor providing electrons at $E^{\circ\prime} < -500$ mV, reductive benzoyl-CoA dearomatization has to be coupled to an exergonic reaction. There are two different solutions for this thermodynamic problem, realized by two different classes of BCRs. The class I and II BCRs differ fundamentally in their amino acid sequence, molecular architecture and cofactor content, but most surprisingly, both yield the identical conjugated dienoyl-CoA product (fig. 2e).

The class I BCR was identified and isolated from the denitrifying *Thauera aromatica* in 1995 [Boll and Fuchs, 1995]; it couples the endergonic reduction of benzoyl-CoA to dienoyl-CoA by a reduced ferredoxin to a stoichiometric

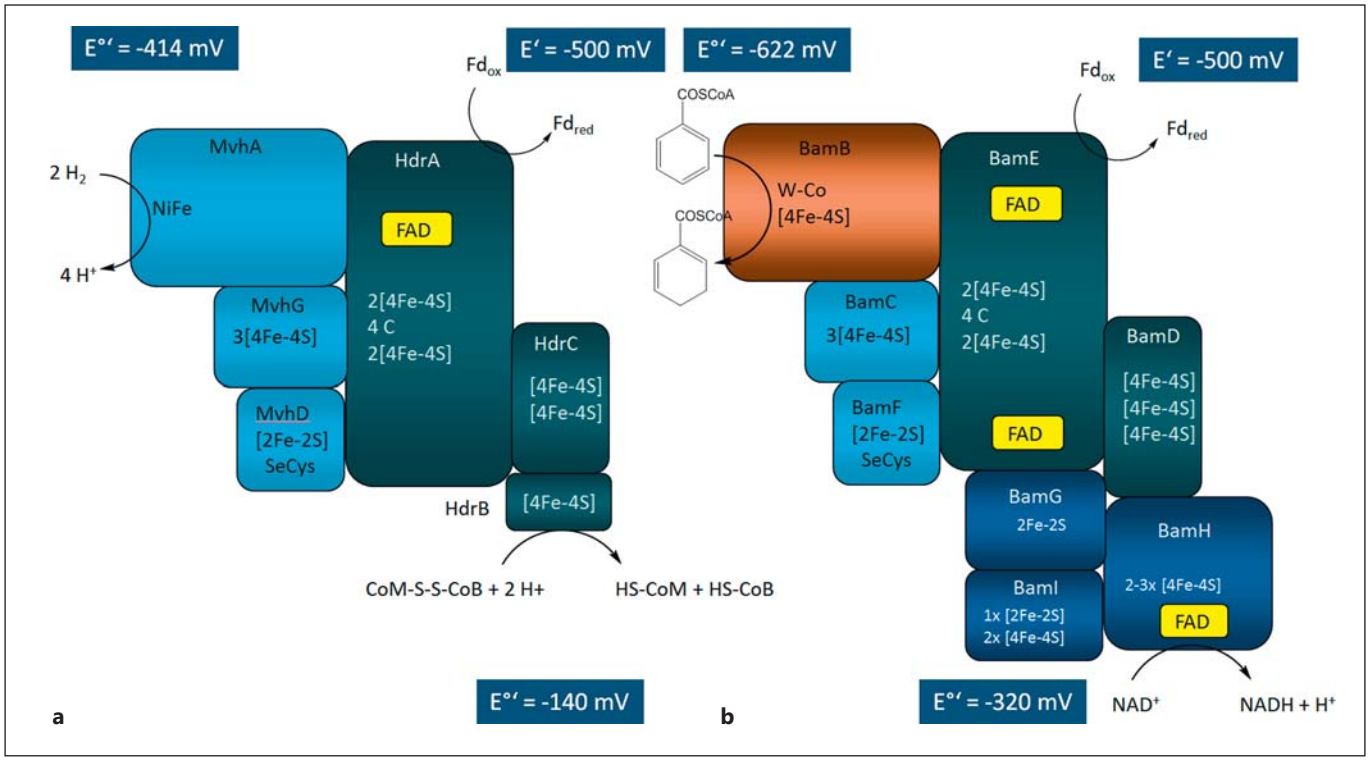

Fig. 5. Schematic subunit architecture/cofactor contents of the hydrogenase/heterodisulfide reductase complex and class II benzoyl-CoA reductase. The interaction of individual components has not been experimentally verified. Subunits depicted in similar colors and sizes indicate amino acid sequence identities >30%. **a** Components of hydrogenase/heterodisulfide reductases from hydrogenotrophic methanogenic archaea. Light blue = Subunits of methyl viologen-reducing hydrogenase (MvhAGD); green = subunits of heterodisulfide reductase (HdrABC). **b** Components of class II benzoyl-CoA reductase (BamBCDEFGHI). Light blue = Components with similarities to MvhGD; green = components with similarities to HdrABC; red = active site component similar to AORs; dark blue = components similar to soluble subunits of complex I (e.g. NuoEFG of *E. coli*). So far, only the BamBC components from *G. metallireducens* have been isolated. For the hydrogenase/heterodisulfide complex, a flavin-based electron bifurcation has experimentally been verified in which endergonic ferredoxin (Fd) reduction by H_2 is driven by the exergonic reduction of the heterodisulfide using the same donor. For class II BCR, an analogous flavin-based electron bifurcation is predicted, in which the endergonic reduction of benzoyl-CoA by reduced ferredoxin is coupled to the exergonic reduction of $NAD(P)^+$ using the same donor. In both, hydrogenase/heterodisulfide reductase and benzoyl-CoA reductase an FAD bound to HdrA/BamE is considered as electron bifurcation cofactor. The 4 C depicted in HdrA means a motif of cysteins conserved with heterodisulfide reductases/BamEs.

ATP hydrolysis (two ATP for the transfer of two electrons [Boll et al., 1997]). Class I BCRs have been found in facultatively anaerobic bacteria and in the aromatic compound degrading archaeon *Ferroglobus placidus* [Holmes et al., 2012; Schmid et al., 2015]. It belongs to the recently introduced BCR/HAD family of radical enzymes that drive low-potential single electron transfer steps to a stoichiometric ATP hydrolysis; they usually contain exclusively [4Fe-4S] clusters as cofactors [Buckel et al., 2014]. Almost 15 years later, an ATP-independent class II BCR was identified as a novel member of the AOR family of bis-WPT-containing enzymes; they appear to be present only in obligately anaerobic bacteria [Kung et al., 2009; Löffler et al., 2011].

General Properties of Class II BCR

Proteomic and transcriptomic analyses of the Fe(III)-respiring *Geobacter metallireducens* identified a benzoate-induced cluster of eight genes, referred to as *bamBCDEFGHI* (benzoic acid metabolism) [Wischgoll et al., 2005]. The corresponding BamBCDEFGHI complex is proposed to have a modular composition (fig. 5b) [Boll et al., 2014]. BamB shows up to 33% amino acid sequence identities to members of the AOR family of W enzymes, and was predicted to contain the site of benzoyl-CoA reduction. The BamCDEF components show sequence identities to components of heterodisulfide reductases and F_{420}-independent hydrogenases of methanogens

(BamCDE, 40–46%; N-terminus of BamF, 55%). They are predicted to contain flavins, numerous FeS clusters and a selenocysteine (BamF). Finally, the putative BamGHI subunits are similar to NADH binding, and flavin/FeS cluster-containing components of NADH:quinone oxidoreductases (e.g. 24–41% to NuoEFG components from *E. coli*). It is predicted that the BamDEFGHI components are involved in a flavin-based electron bifurcation process to accomplish endergonic electron transfer from a low-potential external donor, such as reduced ferredoxin, to the active site [Boll et al., 2014]. This assumption is based on the in vitro evidence for such a flavin-based electron bifurcation in the homologous heterodisulfide-reductase/hydrogenase complex in hydrogenotrophic methanogenic archaea [Buckel and Thauer, 2013]. In *Methanothermobacter marburgensis,* the endergonic reduction of ferredoxin ($E' = -500$ mV) by H_2 ($E^{\circ\prime} = -414$ mV) is driven by the coupling to the exergonic reduction of the CoM-S-S-CoB disulfide ($E^{\circ\prime} = -140$ mV) [Costa et al., 2010; Kaster et al., 2011]. The HdrA component of this complex is similar to BamE, and both are predicted to harbor the electron-bifurcating FAD cofactor. In case of class II BCR, reduction of benzoyl-CoA ($E^{\circ\prime} = -622$ mV) at the active site BamB by an external donor, e.g. a reduced ferredoxin ($E^{\circ\prime} = -500$ mV) could be coupled to the exergonic reduction of a second acceptor, e.g. NAD^+, at the predicted NAD^+-binding BamGHI module (fig. 5b).

Initial attempts to isolate the predicted BamBCDEFGHI complex failed. However, when extracts of *G. metallireducens* grown with benzoate and Fe(III) citrate were treated with 500 mM KCl, a dissociation of the active site BamBC components from the predicted holo enzyme complex was accomplished [Kung et al., 2009]. Based on this protocol, a 185-kDa complex composed of the 73- and 20-kDa BamB and BamC with a $Bam(BC)_2$ architecture was isolated by five chromatographic steps. Predictions from amino acid sequence comparisons, metal analyses and EPR spectroscopy gave rise to the presence of one bis-WPT cofactor, four [4Fe-4S] clusters (one bound to BamB and three to BamC) and a Zn^{2+} per BamBC [Kung et al., 2009].

Kinetic Properties of Class II BCR

Initial attempts to determine a benzoyl-CoA reduction activity of the BamBC-complex in the absence of the putative electron-bifurcating BamDEFGHI components were not successful, even in the presence of low-potential artificial electron donors such as sodium dithionite or Ti(III) citrate. In contrast, BamBC catalyzed the reverse, electron acceptor-dependent oxidation of dienoyl-CoA to benzoyl-CoA, which was routinely used for testing BamBC activity [Kung et al., 2009]. First evidence for the competence of catalyzing the forward reaction was provided by a BamBC-catalyzed isotope exchange reaction, in which the formation of ^{13}C-labeled dienoyl-CoA from a mixture of ring ^{13}C-labeled benzoyl-CoA and nonlabeled dienoyl-CoA was observed [Kung et al., 2010]. Later on, the forward reaction could also be demonstrated by using a combination of Ti(III) citrate and low-potential viologens as mediators; in this case, formation of cyclohex-1-ene-1-carboxyl-CoA (monoenoyl-CoA) was observed, suggesting that the dienoyl-CoA formed was further reduced by two electrons. The observed formation of cyclohexanoyl-CoA might be due to a cyclohexanoyl-CoA dehydrogenase impurity [Kung et al., 2014]. In the absence of an electron acceptor, BamBC catalyzed the disproportionation of two dienoyl-CoA to benzoyl-CoA plus cyclohex-1-enoyl-CoA (monoenoyl-CoA). This activity can be rationalized by the following reaction sequence: (i) two electron transfers to the active site during the oxidation of dienoyl-CoA to benzoyl-CoA; (ii) benzoyl-CoA/dienoyl-CoA exchange, and (iii) reduction of the second bound dienoyl-CoA to monoenoyl-CoA. The low activity and the observed competitive inhibition of BamBC by monoenoyl-CoA ($K_i = 0.2 \pm 0.02$ mM) rather rules out that this disproportionation reaction plays a physiological role [Kung et al., 2010].

In the reverse reaction, BamBC was highly specific for 1,5-dienoyl-CoA, whereas numerous alternative dienoyl- or monoenoyl-CoA analogs were not converted. Moreover, in spite of the similarities to AORs, no oxidation of aldehydes to carboxylic acids was observed in the presence of viologens as electron acceptors. In the oxidized state, BamBC was moderately oxygen sensitive; however, half-life in air dramatically decreased from ≈3 h to 0.5 min in the presence of reducing agents such as dithionite or the dienoyl-CoA product. BamBC was insensitive to cyanide, which typically inactivates Mo/W enzymes that contain inorganic sulfur ligands [Kung et al., 2009]. In contrast, a slight but reproducible activation by 5 mM sodium cyanide was observed. Possible explanations for this stimulatory effect are discussed below.

Structural Properties and Proposed Mechanism of Class II BCR

Overall Structure

The structure of the $Bam(BC)_2$ heterotetramer was recently solved by X-ray crystallography in the as-isolated Zn^{2+}-bound state and in complex with the substrate, product and the inhibitor monoenoyl-CoA based on an-

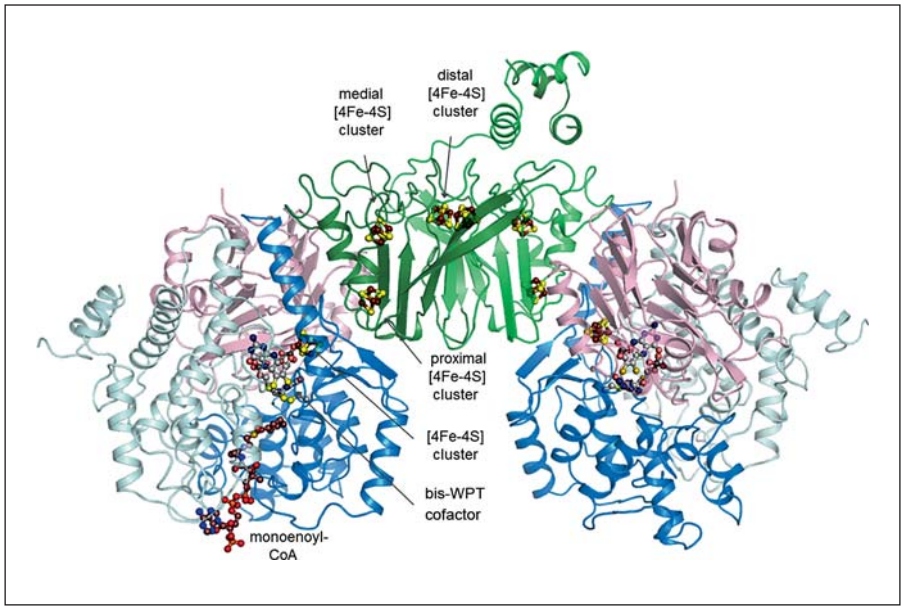

Fig. 6. Overall structure of the Bam(BC)$_2$ subcomplex of class II BCR from *G. metallireducens*. The BamB fold is related to that of AOR and composed of a β-sandwich (1–211) and two helical domains (212–436, 437–653) drawn in pink, marine and light blue. The cofactors are painted as ball-and-stick model. BamC is a ferredoxin-like subunit which was already found as a component in other redox enzymes.

aerobically grown protein crystals [Weinert et al., 2015]. The Bam(BC)$_2$-CoA-ester complex structures are essentially identical at the current resolution and therefore treated as one structural state. The highest resolution of 1.9 Å was obtained for the structure of the Bam(BC)$_2$-inhibitor complex, which was used for fold, W center and substrate binding description. Bam(BC)$_2$ is built up of two central subunits BamC contacting each other and two subunits BamB, each attached to one subunit BamC but not to each other (fig. 6). This architecture suggests two catalytically independent active sites for benzoyl-CoA reduction. However, it also suggests that the electron supply to the two W centers in the Bam(BC)$_2$ complex might be coupled. Similar as other members of the AOR family, BamB is composed of three domains [Chan et al., 1995; Hu et al., 1999] and harbors one bis-WPT cofactor, one Zn atom and one [4Fe-4S] cluster (fig. 6). The electron-transferring BamC subunit has a ferredoxin-like fold and binds three additional [4Fe-4S] clusters. Electrons are transferred over a total distance of more than 40 Å from the distal [4Fe-4S] cluster of BamC to the active site via the [4Fe-4S] clusters of BamC and BamB (fig. 6).

W and Zn Binding Sites

Catalysis of BCRs is predicted to occur in a highly hydrophobic, encapsulated environment to avoid futile electron transfer from the generated low-potential W(IV) electron donor site to solvent-derived protons. In agreement with this assumption, the W center is located in an essentially aprotic and locked cavity in both the 'as-isolated' and CoA-ester-bound states. It is characterized by a distorted octahedral coordination shell which completely shields W and thus prevents binding of an additional ligand (fig. 7). W is coordinated to the four sulfur atoms of the bis-WPT cofactor and two additional ligands. The fifth ligand is a sulfhydryl sulfur of a highly conserved cysteine that is missing in AORs; it, therefore, serves as a distinguishing marker of class II BCRs. A sixth inorganic ligand of the W atom was identified, the nature of which is still unclear [Weinert et al., 2015]. The electron density maps obtained from X-ray structure analysis argue against monoatomic C/N/O ligands, and are in favour of an electron-rich sulfur or chloride ligand (fig. 7). In contrast, extended X-ray absorption fine-structure (EXAFS) analyses at the W L_{III} edge did not support such a scenario. They rather identified, next to the five S atoms, two backscatterers at distances of 2.0 and around 3.2 Å, fitting perfectly to a linear diatomic ligand such as CN^- or CO. In this context, it is remarkable that addition of KCN had a slight but reproducible stimulatory effect on BCR activity. However, Fourier transform infrared spectroscopy, which has frequently been used to detect cyanide ligands bound to Fe atoms in hydrogenases [Pandelia et al., 2010], were not supportive for a W-C≡N bond. Moreover, numerous chemical procedures for detecting cyanide released from denaturated enzyme failed, probably due to the concomitant release of a high amount of sulfide from the [4Fe-4S] clusters. The current discrepancy between

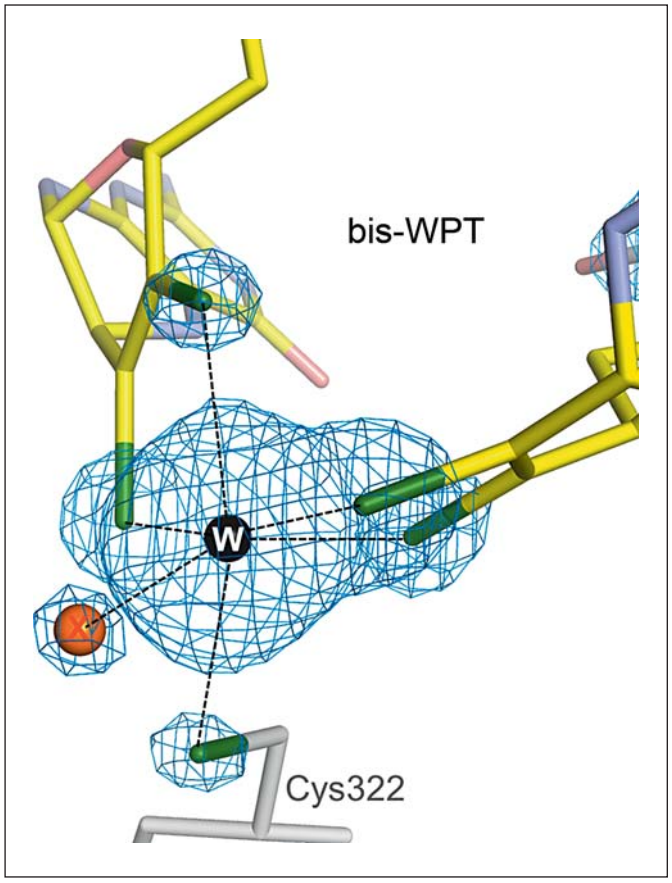

Fig. 7. The structure of the W center. The W is coordinated to the four sulfurs (green) of bis-WPT, one cysteine sulfur and one unknown inorganic ligand (orange) forming a distorted octahedral coordination shell. No open binding site for an additional ligand is present. The contour level of the electron density map is 6σ.

the X-ray and EXFAS data needs further investigations, e.g. by studying enzymes from other organisms.

In agreement with inductively coupled plasma MS, metal analyses and the EXAFS data recorded at the Zn K edge, the as-isolated Bam(BC)$_2$ structure reveals a Zn^{2+} atom 11.5 Å away from W and is not directly involved in the catalytic process (fig. 8). The Zn^{2+} atom is tetrahedrally coordinated by Glu251, His255, Glu257 and His260. These residues are invariant in class II BCRs, suggesting a crucial role of the Zn^{2+} site [Weinert et al., 2015]. Indeed, the Zn^{2+} rigidifies a largely irregular polypeptide segment and contributes to the encapsulation of the active site in the absence of a CoA ester substrate. This shielding property might be essential for protecting the active site for uncontrolled reactions with protons and water.

CoA-Ester Binding

The structures of the Bam(BC)$_2$-CoA ester complexes revealed CoA ester binding inside a long funnel-like channel of 20 Å [Weinert et al., 2015]. CoA ester binding induces the destruction of the Zn^{2+} binding site and the expulsion of the metal from the enzyme as evidenced by X-ray structural and EXAFS data from the two conformational states (fig. 8). In particular, Phe264, Phe323 and Leu434 that occlude the access to the W center in the 'as-isolated' state are displaced upon CoA ester binding. The former Zn^{2+} ligands are rearranged and form a proton storage site that connects the C4 of the substrate with the bulk solvent via a proton transfer pathway. Water molecules cannot reach the substrate in this way, and proton transfer to the W center is blocked by the substrate (fig. 8). In addition, the bound CoA ester takes over the task from the released Zn^{2+} to rigidify the irregular segment. The presence of two alternative Zn- and CoA ester-bound states of BCR was experimentally substantiated by kinetic studies demonstrating the inhibitory effect of supplemental Zn^{2+} with a K_i of 6.7 ± 0.5 μM [Weinert et al., 2015]. The mode of inhibition is not purely competitive, which reflects that Zn^{2+} and the CoA ester substrate bind to different conformations of the enzyme. Due to the usually submicromolar concentration of Zn^{2+} in the cell, the K_d value in the absence of the competing CoA ester is considered to be much lower than the K_i determined.

The six-membered rings of the CoA esters accurately fit into a predominantly hydrophobic cavity (fig. 8). The only hydrophilic residues are His260 and Glu251 that are positioned at a distance of 3.7/3.0 and 4.7/3.9 Å, respectively, apart from C3/C4 of the substrate ring. In particular, His260 serves most likely as proton donor during substrate reduction. The absence of proton donors near C2 or C6 of the substrate ring explains why the enzymatic reduction of the aromatic ring yields the thermodynamically favored conjugated 1,5-dienoyl-CoA. In contrast, the chemical Birch reduction usually proceeds via an 1,4-addition of protons to the aromatic ring resulting in the nonconjugated product [Zimmerman, 2012].

The six-membered ring cannot bind to the ligand-shielded W but lies with a distance of 3.7–4.2 Å nearly in van der Waals distance to its inorganic ligand (fig. 8). Another feature relevant for catalysis are the interactions between the thioester carbonyl of the substrate and Gln466-NE1 and Glu461-OE1, with the carboxylate of the latter being presumably protonated. Notably, the unfavorable geometry of the Glu461 side chain prevents a futile full protonation of the CoA carbonyl that would result in thioester cleavage. The suggested partial protonation of

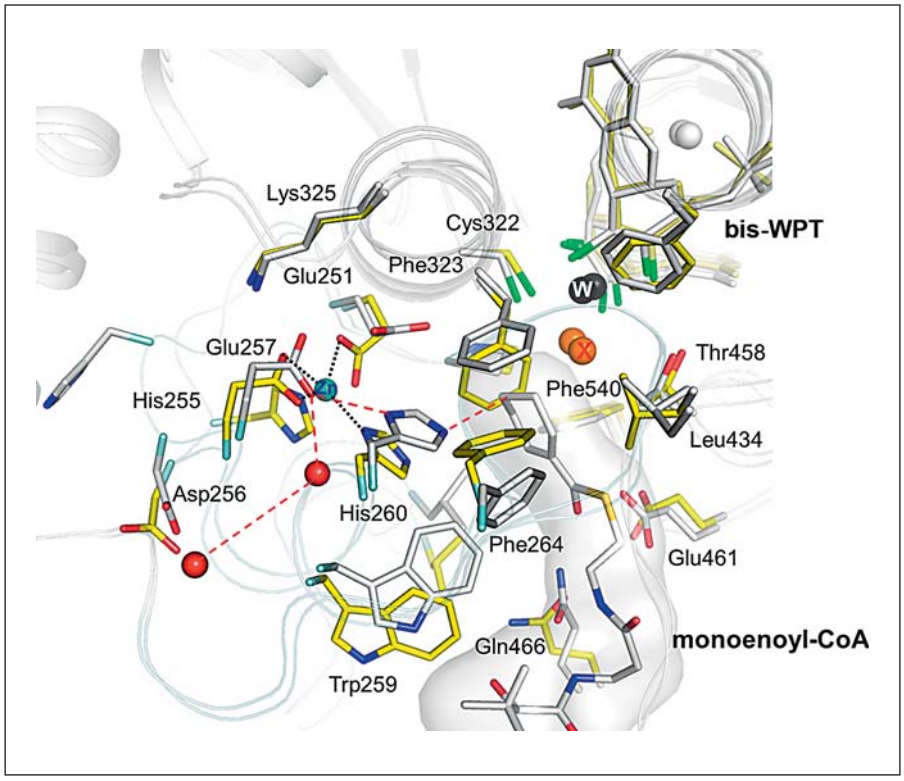

Fig. 8. The as-isolated and CoA ester-bound states of the Bam(BC)$_2$ complex. The superimposed section between the as-isolated (its C in yellow) and CoA ester-bound (its C in gray) Bam(BC)$_2$ structures is focused on the W and Zn binding sites. Monoenoyl-CoA is emphasized by a transparent surface representation. X = Unknown inorganic ligand of W.

the CoA carbonyl is considered to stabilize negatively charged radical/nonradical intermediates during benzene ring reduction.

Catalytic Mechanism

The recent structural insights obtained shed light on the catalytic process of the class II BCR. Two scenarios appear conceivable for class II BCR catalysis: a Birch-like reduction via single electron transfer steps resulting in radical ring intermediates and a nucleophilic aromatic addition presumably via a hydride transfer reaction [Weinert et al., 2015]. The latter implies that the sixth W ligand has to act as a regenerative hydride donor. The following points rather argue for a Birch reduction-like mechanism: (i) The active site of benzoyl-CoA reduction is designed to separate the electron and proton transfer events. A proton storage site is implemented between bulk solvent and the substrate that shuttles protons to the substrate but blocks the access of water. In the absence of the substrates, proton access to the active site is also interrupted via Zn^{2+} binding. (ii) The placement of the substrate ring C4 between the inorganic bis-WPT electron donor ligand and the perfectly positioned, strictly conserved His260 strongly suggests the latter as the favorite proton donor. This arrangement is also consistent with proton-coupled electron transfer steps, a well-known electron transfer principle in enzymology [Weinberg et al., 2012]. In such a scenario, the formation of a highly reactive true radical anion intermediate could be avoided (fig. 9). In contrast, a genuine hydride transfer from the bis-WPT to the C4 suggests the presence of a sulfido or hydroxo ligand at the W; both would be inconsistent with either EXAFS analyses or X-ray structural data. In case of the sixth ligand acting as hydride donor, it has to be regenerated after each turnover. This seems to be only possible by a hardly controllable inflow of water molecules during product/substrate exchange. (iii) A Birch-like mechanism would involve proton-assisted one-electron transfer steps suggesting a W(IV/V) redox chemistry (fig. 9). In agreement with W(IV/V) transitions, BamBC as isolated exhibits a S = 1/2 W(V) EPR signal that disappears upon reduction by dienoyl-CoA to the EPR-silent W(IV) state [Kung et al., 2009].

Distribution/Phylogenetic Tree of BCRs

A W-containing class II BCR has so far only been isolated from the Fe(III)-respiring *G. metallireducens* [Kung et al., 2009]. However, a recent study comprising in vitro

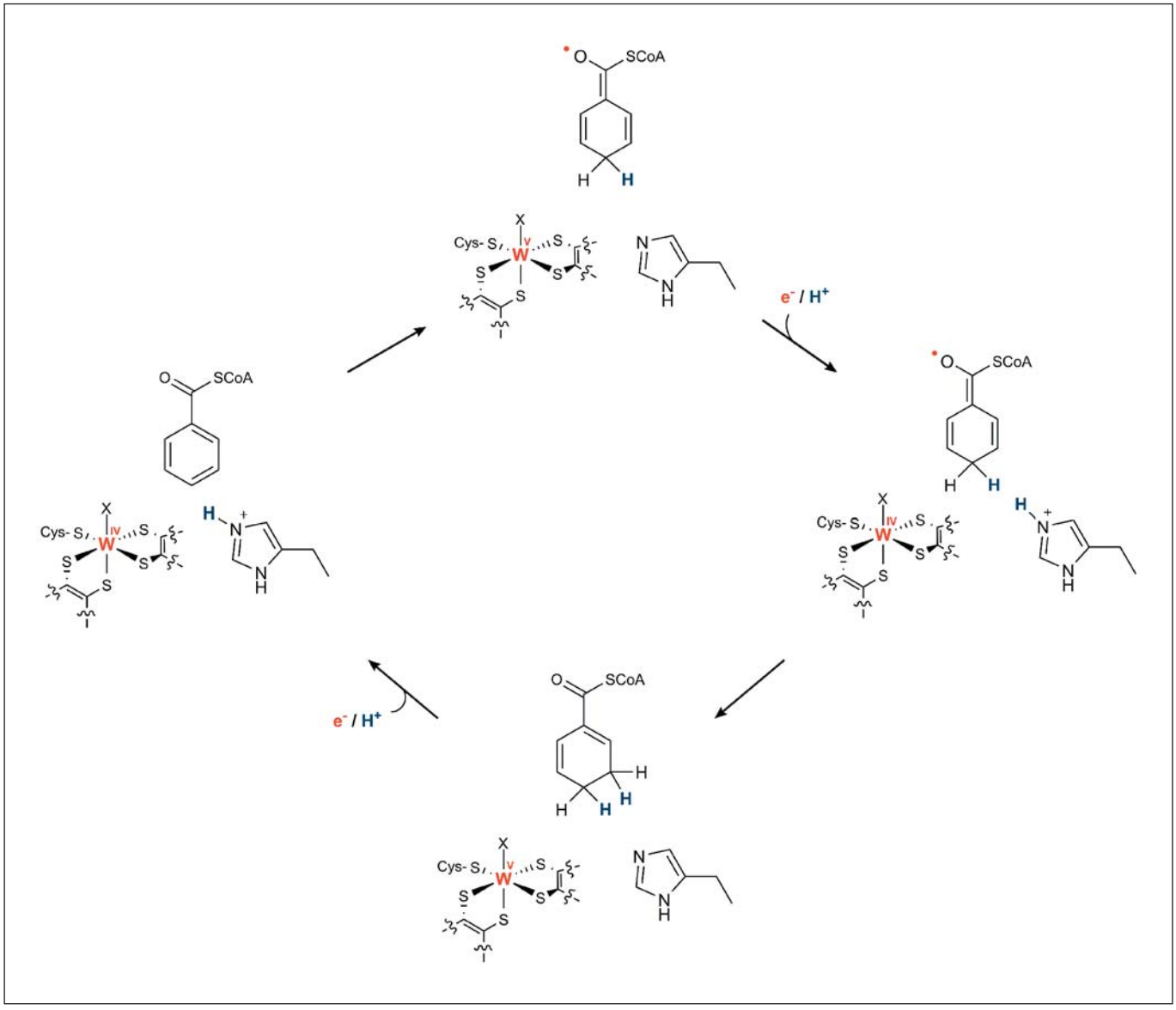

Fig. 9. Proposed proton-coupled electron transfer mechanism of class II benzoyl-CoA reductase catalysis. As an alternative to the ultimate proton donor NE2-His260 shown here, OE2-Glu251 could be involved (not shown).

activity assays as well as gene expression and sequence analyses of the BamB, BamE and BamF components suggested that all obligately anaerobic bacteria with the capacity to degrade aromatic compounds use a class II BCR [Löffler et al., 2011]. Interestingly, all BamF, and in some cases the BamE components, contain a selenocysteine, suggesting that all class II BCRs are W/Se enzymes. The homologous MvhG and HdrA components of methanogenic archaea also often, but not always, contain selenocysteine (fig. 5). Notably, class II BCRs and hydrogenase/heterodisulfide reductase complexes are the only Se-containing enzymes in which selenocysteine is not involved in catalysis at the active site, as it is the case in the W/Se-containing FDH [Hartmann et al., 2014]. The role of selenocysteine in class II BCRs is unknown, and it is unknown whether it can be replaced by a cysteine without a loss of function.

The question arises how the genes encoding BamBs can be identified and distinguished from those encoding AORs? In other words, what are the distinguishing se-

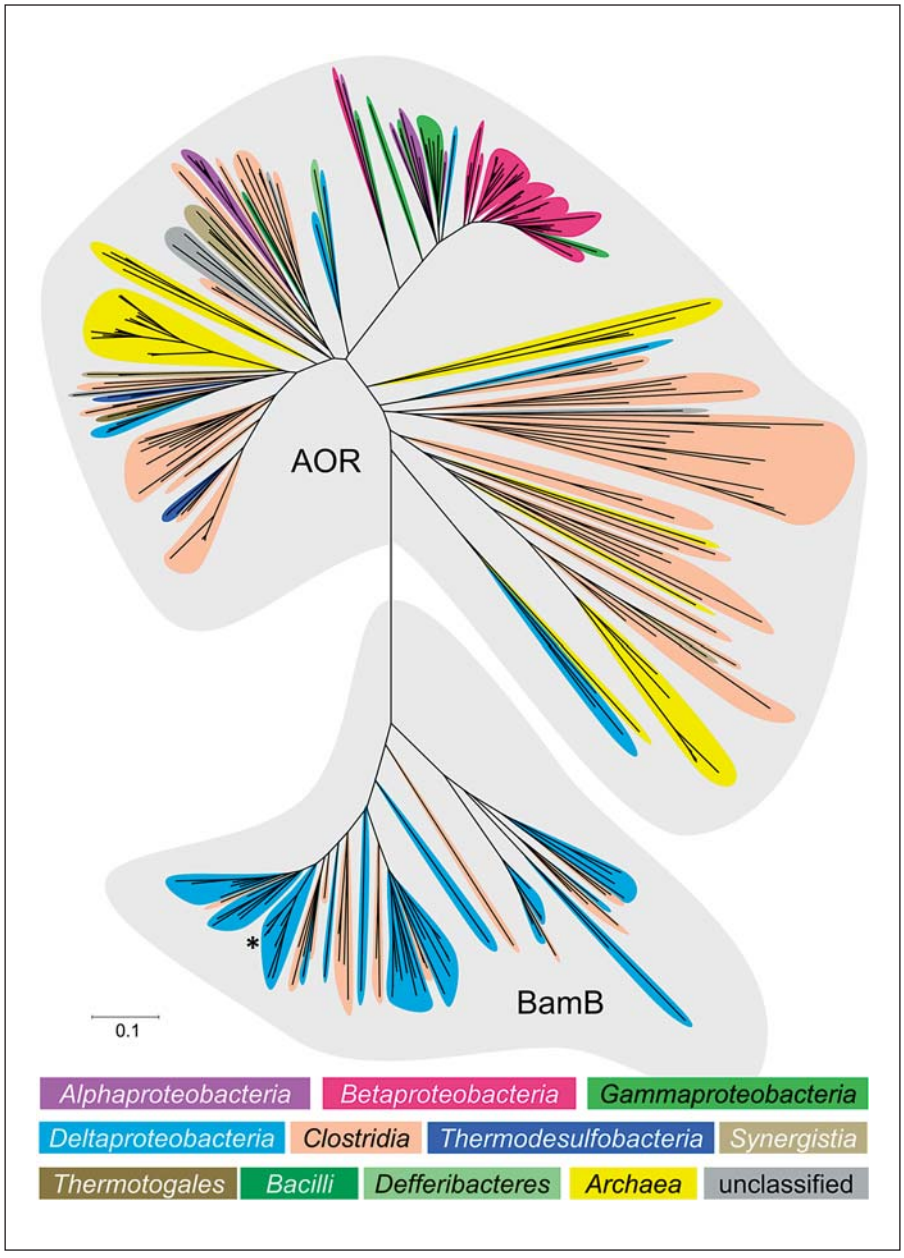

Fig. 10. Phylogenetic tree of the AOR/BamB protein family. The tree was generated from the 326 amino acid sequences with similarities to AORs and BamBs. Taxonomic classes are shown in different colors; for tree generation, BLAST was used (http://blast.ncbi.nlm.nih.gov/Blast.cgi; expect threshold 10; word size 3; max. matches in a query range 0; matrix: BLOSUM62, gap costs: existence, 11, extension: 1). The first 100 sequences obtained for AORs from *Moorella thermoacetica* (GI: 499710967), *Aromatoleum aromaticum* (GI: 499557869) and *Geobacter sulfurreducens* (GI: 504364365) and for BamB from *G. metallireducens* (GI: 490649584, position indicated by asterisk) were combined in one alignment and used in Mega5.2 software (http://megasoftware.net/: neighbor joining; 1,000 bootstrap replications; Poisson model; pairwise deletion of gaps/missing data). The scale bar represents a difference of 0.1 substitutions per site.

quence elements of AORs and BCRs? We suggest the following criteria for a most likely reliable assignment of a gene/polypeptide to a true class II BCR enzyme: (i) amino acid sequence identities higher than 45% to the experimentally verified BamB from *G. metallireducens*; (ii) presence of the conserved cysteine as active site ligand for the W metal (Cys322 in *G. metallireducens* BamB) [Weinert et al., 2015], and (iii) conservation of at least three of the Zn^{2+} ligands (His260, His255, Glu251 and Glu257 in *G. metallireducens* BamB) [Weinert et al., 2015]. Based on these criteria, true BamB components are found in all obligately anaerobic Deltaproteobacteria and Firmicutes that are known to degrade aromatic compounds. These comprise sulfate-reducing, Fe(III)-reducing and fermenting bacteria. An updated phylogenetic tree of BamB clearly indicates that BamB from class II BCRs form a distinct phylogenetic cluster (fig. 10; reference date July 1, 2015).

Class I and II BCRs share the trait of a high oxygen sensitivity [Boll and Fuchs, 1995; Kung et al., 2009], which

explains why they do not occur in aerobic organisms. This property also explains why during anaerobic growth with aromatic compounds oxygen detoxification systems are induced in bacteria containing class I or II BCRs [Heintz et al., 2009; Thiele et al., 2008]. The occurrence of both BCR classes in either facultative or obligate anaerobes is generally explained by the necessary energetic investment for benzene ring dearomatization and the overall yield of energy metabolism. Facultative anaerobes such as denitrifying bacteria or bacteria with an anoxygenic photosynthesis have a much higher ATP yield per aromatic compound oxidized to CO_2 than obligate anaerobes. Therefore, it appeared to be a rule of thumb that they can afford an ATP-dependent irreversible dearomatization step. The relatively simple architecture of class I BCR with [4Fe-4S] clusters as only cofactors and the irreversibility of its reaction enable facultative anaerobes a fast exploitation of aromatic growth substrates in appropriate ecological niches. In contrast, obligate anaerobes, such as sulfate-reducing bacteria, use a reversibly operating enzyme, which is on the one side less energy-consuming, but depends on the other side on numerous metals, uptake systems and biosynthetic cofactor machineries [Boll et al., 2014].

There are some exceptions for the anticipated distribution of class I and II BCRs in facultative and obligate anaerobes, e.g. the obligately anaerobic euryarchaeon *Ferroglobus placidus* uses a class I BCR for the degradation of numerous aromatics such as benzene, toluene or phenol coupled to dissimilatory Fe(III) reduction; the ATP dependence of the enzyme has recently been demonstrated in vitro [Schmid et al., 2015]. Other examples are dearomatizing aryl-CoA reductases from polycyclic aromatic compound-degrading anaerobes, e.g. the sulfate-reducing Deltaproteobacterium NaphS2 or the enrichment culture N47. During growth of these obligate anaerobes with naphthalene, the 2-naphthoyl-CoA intermediate is first reduced to 5,6,7,8-tetrahydro-2-naphthoyl-CoA (THNCoA) by two flavin-dependent reductases belonging to the old yellow enzyme family [Eberlein et al., 2013a; Estelmann et al., 2015]. These enzymes can be regarded as a third class of dearomatizing aryl-CoA reductases [Boll et al., 2014]. The formed THNCoA-CoA is then reduced to a hexahydronaphthoyl-CoA product in an ATP-dependent manner [Eberlein et al., 2013b]. In agreement, the genomes of N47 and NaphS2 contain genes coding fur putative class I BCRs [Bergmann et al., 2011; DiDonato et al., 2010].

Conclusions and Future Perspectives

The W-containing ACH and class II BCR represent two W enzymes catalyzing unprecedented reactions within the Mo/W enzyme families. Both enzyme reactions may be of biotechnological interest: the formation of acetaldehyde from acetylene and cyclic dienes from aromatic rings are important processes to produce valuable building blocks in chemical syntheses. The structural insights into ACH and BCR catalysis provide the prerequisite to future biological or biomimetic synthetic approaches. But there are still a number of open basic questions that need to be addressed in future work.

While ACH, like other members of the DMSOR family, is apparently perfectly suited for redox catalysis, the hydration of C_2H_2 to form acetaldehyde is definitely not a redox reaction. This remarkable finding suggests that an enzyme with a previous redox function was later recruited for the catalysis of the hydration reaction. For the recruitment of ACH as hydrolase, two extreme possibilities may be considered: (i) recruitment may have occurred late after anthropogenic acetylene made its appearance in the world, which would explain the limited distribution in today's biosphere, and (ii) recruitment may have occurred very early when acetylene may have been more abundant. After the disappearance of the primordial source of acetylene, some unknown sources of low-level acetylene would have remained in the environment and microbial acetylene hydration would have been preserved through the ages, albeit with restriction to one or a few species in special niches [Wächtershäuser, pers. commun.]. So far, ACH has only been isolated and structurally characterized from the Deltaproteobacterium *P. acetylenicus*. It exhibits a remarkable specificity for acetylene; other potential substrates, such as N_2, CO and derivatives of acetylene, are not converted. This finding supports the idea that ACH is an ancient enzyme that evolved in an early phase of biochemical evolution when acetylene was more abundant in the Earth's atmosphere [Culbertson et al., 1988]. At this point, a definitive reaction mechanism cannot be formulated in detail despite the availability of a high-resolution X-ray structure and several computational studies to model the reaction pathway.

In case of class II BCR, one of the most intriguing open questions is the nature of the sixth inorganic ligand at the W atom. As the outer shell electron transfer from the reduced W metal has to occur via this ligand to the aromatic ring, its unambiguous identification will be the key to understand the catalytic function of the enzyme. In particular EXAFS data favor a diatomic sixth ligand,

most probably cyanide. However, a W-cyanide bond would be unprecedented in nature, and its clear identification needs numerous future spectroscopic and structural analyses, most probably with enzymes from different organisms. In any case, the transfer of two single electrons from the Mo/W metal via a ligand to the substrate without binding of the latter to the metal is unique among MPT/WPT-containing enzymes. The huge number of *bamB*-like genes in genomes from Deltaproteobacteria and Firmicutes (<45% sequence identity) poses the question whether all of these code for class II BCR or for enzymes with different, so far unknown, functions.

Another open question is the mode of energetic coupling in class II BCRs. The obvious similarities of the BamCDEF modules to components of electron bifurcating hydrogenase/heterodisulfide complexes from hydrogenotrophic methanogens suggest a similar mode of energetic coupling in these enzymes. However, experimental evidence for the predicted coupling of the endergonic benzoyl-CoA reduction to the exergonic NAD^+ reduction with a reduced ferredoxin as medium-potential electron donor has not been shown yet. Most possibly, the demonstration of such or a similar process will rely on the availability of a pure, intact holo enzyme complex to exclude intervening short-cut electron transfer reactions in cell extracts.

Acknowledgements

This work was funded by the DFG (Deutsche Forschungsgemeinschaft) within the framework of the Scientific Priority Programme SPP1319 – 'Biological transformation of hydrocarbons without oxygen: from the molecular to the global scale'.

References

Abbasian F, Lockington R, Mallavarapu M, Naidu R: A comprehensive review of aliphatic hydrocarbon biodegradation by bacteria. Applied Biochem Biotechnol 2015;176:670–699.

Abt DJ: Tungsten-Acetylene Hydratase from *Pelobacter acetylenicus* and Molybdenum-Transhydroxylase from *Pelobacter acidigallici*. Two Novel Molybdopterin and Iron-Sulfur Containing Enzymes; thesis, University of Konstanz, 2001.

Andreesen JR, Makdessi K: Tungsten, the surprisingly positively acting heavy metal element for prokaryotes. Ann NY Acad Sci 2008;1125:215–229.

Bas DC, Rogers DM, Jensen JH: Very fast prediction and rationalization of pKa values for protein-ligand complexes. Proteins 2008;73:765–783.

Bashford D, Karplus M: pKa's of ionizable groups in proteins: atomic detail from a continuum electrostatic model. Biochemistry 1990;29:10219–10225.

Bergmann F, Selesi D, Weinmaier T, Tischler P, Rattei T, Meckenstock RU: Genomic insights into the metabolic potential of the polycyclic aromatic hydrocarbon degrading sulfate-reducing Deltaproteobacterium N47. Environ Microbiol 2011;13:1125–1137.

Beroza P, Fredkin DR, Okamura MY, Feher G: Protonation of interacting residues in a protein by a Monte Carlo method: application to lysozyme and the photosynthetic reaction center of *Rhodobacter sphaeroides*. Proc Natl Acad Sci USA 1991;88:5804–5808.

Bevers LE, Hagedoorn PL, Hagen WR: The bioinorganic chemistry of tungsten. Coord Chem Rev 2009;253:269–290.

Birch AJ: Reduction by dissolving metals. Part I. J Chem Soc 1944, pp 430–436.

Birch-Hirschfeld L: Die Umsetzung von Acetylen durch *Mycobacterium lacticola*. Zentralbl Bakteriol Parasitenk 1932;86:113–129.

Boll M: Dearomatizing benzene ring reductases. J Mol Microbiol Biotechnol 2005;10:132–142.

Boll M, Albracht SS, Fuchs G: Benzoyl-CoA reductase (dearomatizing), a key enzyme of anaerobic aromatic metabolism. A study of adenosinetriphosphatase activity, ATP stoichiometry of the reaction and EPR properties of the enzyme. Eur J Biochem 1997;244:840–851.

Boll M, Fuchs G: Benzoyl-coenzyme A reductase (dearomatizing), a key enzyme of anaerobic aromatic metabolism. ATP dependence of the reaction, purification and some properties of the enzyme from *Thauera aromatica* strain K172. Eur J Biochem 1995;234:921–933.

Boll M, Fuchs G, Meier C, Trautwein A, El Kasmi A, Ragsdale SW, Buchanan G, Lowe DJ: Redox centers of 4-hydroxybenzoyl-CoA reductase, a member of the xanthine oxidase family of molybdenum-containing enzymes. J Biol Chem 2001;276:47853–47862.

Boll M, Löffler C, Morris BE, Kung JW: Anaerobic degradation of homocyclic aromatic compounds via arylcarboxyl-coenzyme A esters: organisms, strategies and key enzymes. Environ Microbiol 2014;16:612–627.

Boll M, Schink B, Messerschmidt A, Kroneck PMH: Novel bacterial molybdenum and tungsten enzymes: three-dimensional structure, spectroscopy, and reaction mechanism. Biol Chem 2005;386:999–1006.

Bombarda E, Ullmann GM: pH-dependent pK_a values in proteins – a theoretical analysis of protonation energies with practical consequences for enzymatic reactions. J Phys Chem 2010;114:1994–2003.

Buckel W, Kung JW, Boll M: The benzoyl-coenzyme A reductase and 2-hydroxyacyl-coenzyme A dehydratase radical enzyme family. ChemBioChem 2014;15:2188–2194.

Buckel W, Thauer RK: Energy conservation via electron bifurcating ferredoxin reduction and proton/Na(+) translocating ferredoxin oxidation. Biochim Biophys Acta 2013;1827:94–113.

Carmona M, Zamarro MT, Blazquez B, Durante-Rodriguez G, Juarez JF, Valderrama JA, Barragan MJ, Garcia JL, Diaz E: Anaerobic catabolism of aromatic compounds: a genetic and genomic view. Microbiol Mol Biol Rev 2009;73:71–133.

Chan MK, Mukund S, Kletzin A, Adams MW, Rees DC: Structure of a hyperthermophilic tungstopterin enzyme, aldehyde ferredoxin oxidoreductase. Science 1995;267:1463–1469.

Costa KC, Wong PM, Wang T, Lie TJ, Dodsworth JA, Swanson I, Burn JA, Hackett M, Leigh JA: Protein complexing in a methanogen suggests electron bifurcation and electron delivery from formate to heterodisulfide reductase. Proc Natl Acad Sci USA 2010;107:11050–11055.

Culbertson CW, Strohmaier FE, Oremland RS: Acetylene as a substrate in the development of primordial bacterial communities. Orig Life Evol Biosph 1988;18:397–340.

de Bont JAM, Peck MW: Metabolism of acetylene by *Rhodococcus* A1. Arch Microbiol 1980;127:99–104.

DiDonato RJ Jr, Young ND, Butler JE, Chin KJ, Hixson KK, Mouser P, Lipton MS, DeBoy R, Methe BA: Genome sequence of the deltaproteobacterial strain NaphS2 and analysis of differential gene expression during anaerobic growth on naphthalene. PLoS One 2010;5:e14072.

Dobbek H, Huber R: The molybdenum and tungsten cofactors: a crystallographic view. Metal Ions Biol Syst 2002;39:227–263.

Eberlein C, Estelmann S, Seifert J, von Bergen M, Müller M, Meckenstock RU, Boll M: Identification and characterization of 2-naphthoyl-coenzyme A reductase, the prototype of a novel class of dearomatizing reductases. Mol Microbiol 2013a;88:1032–1039.

Eberlein C, Johannes J, Mouttaki H, Sadeghi M, Golding BT, Boll M, Meckenstock RU: ATP-dependent/-independent enzymatic ring reductions involved in the anaerobic catabolism of naphthalene. Environ Microbiol 2013b;15:1832–1841.

Einsle O, Niessen H, Abt DJ, Seiffert GB, Schink B, Huber R, Messerschmidt A, Kroneck PMH: Crystallization and preliminary X-ray analysis of the tungsten-dependent acetylene hydratase from *Pelobacter acetylenicus*. Acta Crystallogr Sect F Struct Biol Cryst Commun 2005;61:299–301.

Estelmann S, Blank I, Feldmann A, Boll M: Two distinct old yellow enzymes are involved in naphthyl ring reduction during anaerobic naphthalene degradation. Mol Microbiol 2015;95:162–172.

Fuchs G, Boll M, Heider J: Microbial degradation of aromatic compounds – from one strategy to four. Nat Rev Microbiol 2011;9:803–816.

Hartmann T, Schwanhold N, Leimkühler S: Assembly and catalysis of molybdenum or tungsten-containing formate dehydrogenases from bacteria. Biochim Biophys Acta 2014;1854:1090–1100.

Heintz D, Gallien S, Wischgoll S, Ullmann AK, Schaeffer C, Kretzschmar AK, van Dorsselaer A, Boll M: Differential membrane proteome analysis reveals novel proteins involved in the degradation of aromatic compounds in *Geobacter metallireducens*. Mol Cell Proteomics 2009;8:2159–2169.

Hille R: The molybdenum oxotransferases and related enzymes. Dalton Trans 2013;42:3029–3042.

Hille R, Hall J, Basu P: The mononuclear molybdenum enzymes. Chem Rev 2014;114:3963–4038.

Holmes DE, Risso C, Smith JA, Lovley DR: Genome-scale analysis of anaerobic benzoate and phenol metabolism in the hyperthermophilic archaeon *Ferroglobus placidus*. ISME J 2012;6:146–157.

Hu Y, Faham S, Roy R, Adams MW, Rees DC: Formaldehyde ferredoxin oxidoreductase from *Pyrococcus furiosus*: the 1.85 Å resolution crystal structure and its mechanistic implications. J Mol Biol 1999;286:899–914.

Hyman MR, Arp DJ: Acetylene inhibition of metalloenzymes. Anal Biochem 1988;173:207–220.

Kanner D, Bartha R: Growth of *Nocardia rhodochrous* on acetylene gas. J Bacteriol 1979;139:225–230.

Kaster AK, Moll J, Parey K, Thauer RK: Coupling of ferredoxin and heterodisulfide reduction via electron bifurcation in hydrogenotrophic methanogenic archaea. Proc Natl Acad Sci USA 2011;108:2981–2986.

Kletzin A, Adams MW: Tungsten in biological systems. FEMS Microbiol Rev 1996;18:5–63.

Klingen AR, Bombarda E, Ullmann GM: Theoretical investigation of the behavior of titratable groups in proteins. Photochem Photobiol Sci 2006;5:588–596.

Kung JW, Meier AK, Mergelsberg M, Boll M: Enzymes involved in a novel anaerobic cyclohexane carboxylic acid degradation pathway. J Bacteriol 2014;196:3667–3674.

Kung JW, Baumann S, von Bergen M, Müller M, Hagedoorn PL, Hagen WR, Boll M: Reversible biological Birch reduction at an extremely low redox potential. J Am Chem Soc 2010;132:9850–9856.

Kung JW, Löffler C, Dorner K, Heintz D, Gallien S, Van Dorsselaer A, Friedrich T, Boll M: Identification and characterization of the tungsten-containing class of benzoyl-coenzyme A reductases. Proc Natl Acad Sci USA 2009;106:17687–17692.

Liao R-Z, Thiel W: Comparison of QM-only and QM/MM models for the mechanism of tungsten-dependent acetylene hydratase. J Chem Theory Comput 2012;8:3793–3803.

Liao R-Z, Thiel W: Convergence in the QM-only and QM/MM modeling of enzymatic reactions: a case study for acetylene hydratase. J Comput Chem 2013;34:2389–2397.

Liao R-Z, Yu J-G, Himo F: Mechanism of tungsten-dependent acetylene hydratase from quantum chemical calculations. Proc Natl Acad Sci USA 2010;52:22523–22527.

Löffler C, Kuntze K, Vazquez JR, Rugor A, Kung JW, Böttcher A, Boll M: Occurrence, genes and expression of the W/Se-containing class II benzoyl-coenzyme A reductases in anaerobic bacteria. Environ Microbiol 2011;13:696–709.

L'vov NP, Nosikov AN, Antipov AN: Tungsten-containing enzymes. Biochemistry (Mosc) 2002;67:196–200.

Meckenstock RU, Krieger R, Ensign S, Kroneck PMH, Schink B: Acetylene hydratase of *Pelobacter acetylenicus*. Molecular and spectroscopic properties of the tungsten iron-sulfur enzyme. Eur J Biochem 1999;264:176–182.

Miller LG, Baesman SM, Kirshtein J, Voytek MA, Oremland RS: A biogeochemical and genetic survey of acetylene fermentation by environmental samples and bacterial isolates. Geomicrobiol J 2013;30:501–516.

Mobitz H, Boll M: A Birch-like mechanism in enzymatic benzoyl-CoA reduction: a kinetic study of substrate analogues combined with an *ab initio* model. Biochemistry 2002;41:1752–1758.

Onufriev A, Case DA, Ullmann GM: A novel view of pH titration in biomolecules. Biochemistry 2001;40:3413–3419.

Oremland RS, Voytek MA: Acetylene as fast food: implications for development of life on anoxic primordial Earth and in the outer solar system. Astrobiology 2008;8:45–58.

Pandelia ME, Ogata H, Lubitz W: Intermediates in the catalytic cycle of [NiFe] hydrogenase: functional spectroscopy of the active site. ChemPhysChem 2010;11:1127–1140.

Pushie MJ, Cotelesage JJ, George GN: Molybdenum and tungsten oxygen transferases – and functional diversity within a common active site motif. Metallomics 2014;6:15–24.

Romao MJ: Molybdenum and tungsten enzymes: a crystallographic and mechanistic overview. Dalton Trans 2009;7:4053–4068.

Rosner BM, Rainey FA, Kroppenstedt RM, Schink B: Acetylene degradation by new isolates of aerobic bacteria and comparison of acetylene hydratase enzymes. FEMS Microbiol Lett 1997;148:175–180.

Rosner BM, Schink B: Purification and characterization of acetylene hydratase of *Pelobacter acetylenicus*, a tungsten iron-sulfur protein. J Bacteriol 1995;177:5767–5772.

Rothery RA, Weiner JH: Shifting the metallocentric molybdoenzyme paradigm: the importance of pyranopterin coordination. J Biol Inorg Chem 2015;20:349–372.

Roy R, Adams MW: Tungsten-dependent aldehyde oxidoreductase: a new family of enzymes containing the pterin cofactor. Met Ions Biol Syst 2002;39:673–697.

Schink B: Fermentation of acetylene by an obligate anaerobe, *Pelobacter acetylenicus* sp. nov. Arch Microbiol 1985;142:295–301.

Schink B: The genus Pelobacter; in Dworkin M, Falkow S, Rosenberg E, Schleifer K-H, Stackebrandt E (eds): The Prokaryotes. New York, Springer, 2006, vol 3, pp 5–11.

Schmid G, Rene SB, Boll M: Enzymes of the benzoyl-coenzyme A degradation pathway in the hyperthermophilic archaeon *Ferroglobus placidus*. Environ Microbiol 2015:17:3289–3000.

Schmidt A, Frensch M, Schleheck D, Schink B, Müller N: Degradation of acetaldehyde and its precursors by *Pelobacter carbinolicus* and *P. acetylenicus*. PLoS One 2014;9:e115902.

Schwarz G, Mendel RR, Ribbe MW: Molybdenum cofactors, enzymes and pathways. Nature 2009;460:839–847.

Seiffert G: Structural and Functional Studies on Two Molybdopterin and Iron-Sulfur Containing Enzymes: Transhydroxylase from *Pelobacter acidigallici* and Aceytlene Hydratase from *Pelobacter acetylenicus*; thesis, University of Konstanz, 2007.

Seiffert GB, Abt D, Ten Brink F, Fischer D, Einsle O, Kroneck PMH: Acetylene hydratase; in Messerschmidt A (ed): Handbook of Metalloproteins. Chichester, Wiley, 2008, vol 4/5, pp 541–548.

Seiffert GB, Ullmann GM, Messerschmidt A, Schink B, Kroneck PM, Einsle O: Structure of the non-redox-active tungsten/[4Fe:4S] enzyme acetylene hydratase. Proc Natl Acad Sci USA 2007;104:3073–3077.

Stewart LJ, Bailey S, Bennett B, Charnock JM, Garner CD, McAlpine AS: Dimethylsulfoxide reductase: an enzyme capable of catalysis with either molybdenum or tungsten at the active site. J Mol Biol 2000;299:593–600.

Stewart WD, Fitzgerald GP, Burris RH: In situ studies on N_2 fixation using the acetylene reduction technique. Proc Natl Acad Sci 1967; 58:2071–2078.

Sudmeier JL, Reilley CN: Nuclear magnetic resonance studies of protonation of polyamine and aminocarboxylate compounds in aqueous solution. Anal Chem 1964;36:1698–1706.

Ten Brink F: Acetylene Hydratase from *Pelobacter acetylenicus*. Functional Studies on a Gas-Processing Tungsten, Iron-Sulfur Enzyme by Site Directed Mutagenesis and Crystallography; thesis, University of Konstanz, 2010.

Ten Brink F: Living on acetylene. A primordial energy source. Met Ions Life Sci 2014;14:15–35.

Ten Brink F, Schink B, Kroneck PMH: Exploring the active site of the tungsten, iron-sulfur enzyme acetylene hydratase. J Bacteriol 2011; 193:1229–1236.

Thiele B, Rieder O, Jehmlich N, von Bergen M, Müller M, Boll M: Aromatizing cyclohexa-1,5-diene-1-carbonyl-coenzyme A oxidase. Characterization and its role in anaerobic aromatic metabolism. J Biol Chem 2008; 283:20713–20721.

Ullmann GM, Bombarda E: pK_a values and redox potentials of proteins. What do they mean? Biol Chem 2013;394:611–619.

Ullmann GM, Bombarda E: Continuum electrostatic analysis of proteins; in Náray-Szabó G (ed): Protein Modelling. Berlin, Springer, 2014, pp 135–163.

Ullmann GM, Knapp E-W: Electrostatic computations of protonation and redox equilibria in proteins. Eur Biophys J 1999;28:533–551.

Ullmann RT, Ullmann GM: GMCT: a Monte Carlo simulation package for macromolecular receptors. J Comput Chem 2012;33:887–900.

Unciuleac M, Warkentin E, Page CC, Boll M, Ermler U: Structure of a xanthine oxidase-related 4-hydroxybenzoyl-CoA reductase with an additional [4Fe-4S] cluster and an inverted electron flow. Structure 2004;12:2249–2256.

Vorholt JA, Thauer RK: Molybdenum and tungsten enzymes in C1 metabolism. Met Ions Biol Syst 2002;39:571–619.

Weinberg DR, Gagliardi CJ, Hull JF, Murphy CF, Kent CA, Westlake BC, Paul A, Ess DH, McCafferty DG, Meyer TJ: Proton-coupled electron transfer. Chem Rev 2012;112:4016–4093.

Weinert T, Huwiler SG, Kung JW, Weidenweber S, Hellwig P, Stärk H-J, Biskup T, Cotelesage JJH, George GN, Ermler U, Boll M: Structural basis of enzymatic benzene ring reduction. Nat Chem Biol 2015;11:586–591.

Wischgoll S, Heintz D, Peters F, Erxleben A, Sarnighausen E, Reski R, Van Dorsselaer A, Boll M: Gene clusters involved in anaerobic benzoate degradation of *Geobacter metallireducens*. Mol Microbiol 2005;58:1238–1252.

Zimmerman HE: A mechanistic analysis of the Birch reduction. Acc Chem Res 2012;45:164–170.